

Improved algorithms for determining the strain of optical fibers using Brillouin reflectometers

I V Bogachkov

Omsk State Technical University, 11, Mira Ave., Omsk, 644050, Russia

E-mail: bogachkov@mail.ru

Abstract. The issues of improved algorithms for determining the strain of optical fibers using Brillouin reflectometers are investigated. Structure charts of devices for early diagnostics of optical fibers are presented. Adaptive algorithms for construction of Brillouin reflectograms: patterns of Brillouin frequency shift and strain distribution along the optical waveguide are considered. Reference Brillouin reflectograms for different optical fibers from the database are required to correctly detect the “problem” segments (segments of optical fibers with increased mechanical strain or with transformed temperature) in the optical waveguide.

Index Terms. Optical fiber, strain, Mandelstam – Brillouin scattering, Brillouin reflectometer, Brillouin frequency shift.

1. Introduction

Fiber optical communication lines (FOCL) are widely used in modern infocommunication systems. Tasks of monitoring and early diagnostics of optical fibers (OF) are important for companies operating FOCL [1, 2].

Timely detection and elimination of potentially hazardous segments in an OF (segments with bends, cracks (defects), increased mechanical strain and transformed temperature, with different types of unauthorized access to the OF) are required to avoid the gradual degradation and destruction of the OF in FOCL [2, 3].

Specialized device – Brillouin optical time domain reflectometer (BOTDR) can be used for early diagnostics of OFs located in the laid optical cables (OCs) [2 – 7]. This BOTDR is needed to detect OF segments with increased longitudinal strain and transformed temperature. Usual optical time domain reflectometers (OTDRs) are unfit for such tasks, because backscattered Rayleigh scattering signal is analyzed in them, a frequency of which is equal to a frequency of a probe radiation. In contrast, in the BOTDR a backscattered signal containing components of the Mandelstam – Brillouin scattering (MBS) is analyzed [2 – 4].

Receiving a distribution pattern of a Mandelstam – Brillouin backscatter spectrum (MBBS) along an OF (3D-BOTDR reflectogram of MBBS distribution) we find a Brillouin frequency shift (f_B). After that, a distribution pattern of the strain is constructed along the OF [2, 3].

The attractive feature of the BOTDR (compared with other devices for determining the strain in an OF) is one-end access to the OF.

The process of determining the f_B in the OF and then the longitudinal OF strain is very slow. Therefore, the task of improving the structure charts of devices for early diagnostics of FOCL and processing algorithms to accelerate a production of final results is important.



The work was carried out with the financial support of the Ministry of Education and Science of the Russian Federation within the scope of the base part of a State Assignment within the sphere of scientific activity (Project No. 8.9334.2017/8.9).

2. The theory

In the traditional structure chart of the BOTDR either a frequency of radiation introduced into the OF (a frequency of the emitting laser in transmission path) changes, which is necessary to simplify a receive path, since it will be configured to receive the backscattered signal with fixed frequency [3]. Or tuning of the receive path in frequency of the backscattered signal is carried out, which allows us to do without tuning a frequency of an emitting laser in the transmission path [4].

Fig. 1 shows the structure chart for the first case, and Fig. 2 – for the second.

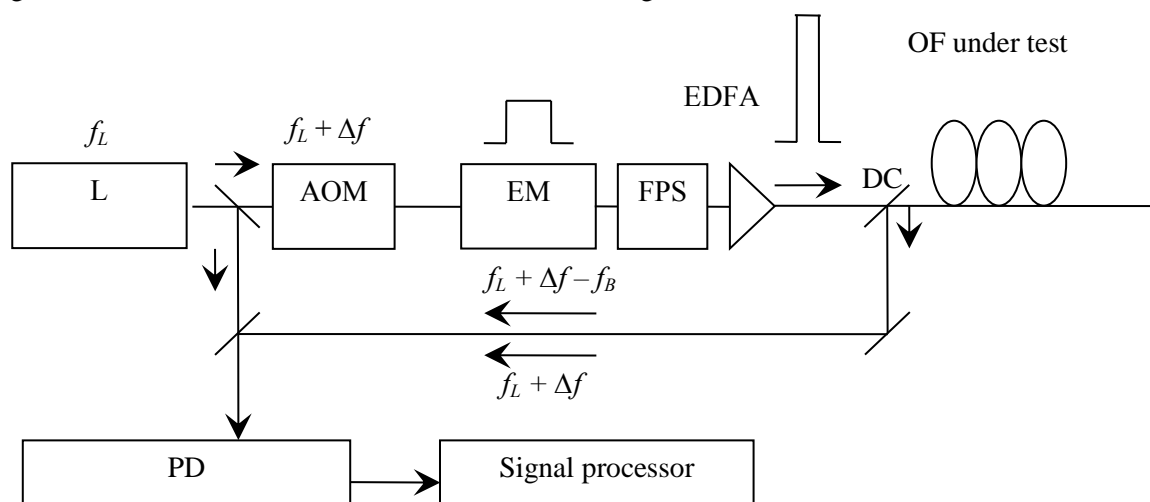


Figure 1. Simplified structure chart of BOTDR

The emitting source is a laser diode (L) (f_L is the frequency of emitting laser in the transmission path); the frequency shift (Δf) is carried out by an acousto-optical modulator (AOM); the pulse modulation is made by an electro-absorption modulator (EM). After polarization change in the Faraday phase shifter (FPS) the optical signal is amplified in the erbium-doped fiber amplifier (EDFA) and then it is supplied to the OF under test through a directional coupler (DC) or a circulator.

The backscattered optical signal is guided to the photodetector (PD) through a DC or circulator. This signal consists of both a component of Rayleigh scattering (a frequency is equal to a radiation frequency in the transmission path ($f_L + \Delta f$)) and two components of MBS (Stokes and anti-Stokes). The Stokes component is shifted downwards in frequency ($f_L + \Delta f - f_B$), and the anti-Stokes component is shifted upwards ($f_L + \Delta f + f_B$). Coherent radiation reception is used to isolate the Stokes component (more powerful). A smaller part of the laser radiation power is supplied to the PD input, where it is mixed with the radiation scattered in the OF.

Coherent reception is used to increase the sensitivity of the PD. In comparison with the direct detection chart applied in traditional OTDR the improvement is about 10 – 20 dB [2 – 4].

An addition, it is necessary to apply more sensitive PD in BOTDR (in comparison with OTDR) because a coefficient of spontaneous MBS about 14 dB is less than a coefficient of Rayleigh scattering [1 – 3].

A 3D-distribution of spectrum of the spontaneous MBS along the optical waveguide is found for each frequency $f_L + \Delta f$, and then a “peak” frequency of the MBBS is determined. After determining the f_B ,

the strain distribution along the OF is calculated. A peak signal level in PD (MBBS maximum) is achieved when the AOM frequency shift (Δf) is f_B .

A more popular structure chart with fixed transmission path used in the BOTDR “Ando AQ 8603” is depicted in Fig. 2 [4].

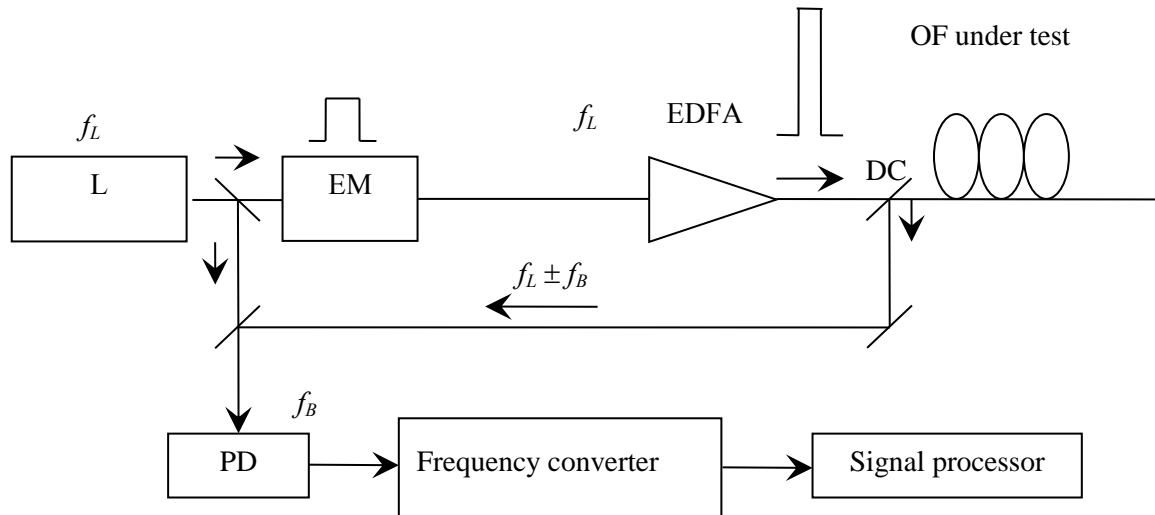


Figure 2. Simplified structure chart of BOTDR

The MBBS profile along the optical waveguide is determined by separating the difference between the f_L frequency and the spectrum frequencies of the backscattered signal in the receive path. The difference frequencies (corresponding to MBBS) occupy a band from 9.5 GHz to 11.4 GHz at a wavelength of $1.55 \mu\text{m}$ (λ_L) of the emitting laser. After that, in the frequency converter usually performed as a heterodyne scheme the frequency of the scan range under study is reduced to the threshold that allows digital signal processing in the signal processor to be performed.

Also, there are other types of structure charts of BOTDR [5 – 7].

For instance, it is possible to use Rayleigh reflectogram for analysis as well as in OTDR [5], and also the introduction of a reference channel containing either an OF in the reference receive channel [6] or a reference reflectogram from the database of different OF types [7, 12 – 14].

As is known, the frequency profile of MBBS ($g_B(f)$ – Brillouin gain coefficient, (BGC)) has a “Lorentzian profile” (parabolic shape) in the region of the main maximum (“peak”):

$$g_B = \frac{g_{B0}}{1 + \left(\frac{f_L - f - f_B}{\Delta f_B / 2} \right)^2}, \quad (1)$$

where g_{B0} is the maximum BGC at the $f = f_L - f_B$; Δf_B is the bandwidth of the MBBS (Brillouin gain) [2 – 4].

The relation of the MBBS peak shift Δf_B and the intensity of the anti-Stokes wave ΔI with changes in Young’s module (strain) ΔE_ε and temperature ΔT can be expressed by matrix form:

$$\begin{bmatrix} \Delta f_B (\Delta E_\varepsilon, \Delta T) \\ \Delta I (\Delta E_\varepsilon, \Delta T) \end{bmatrix} = \begin{bmatrix} C_f^\varepsilon & C_f^T \\ C_I^\varepsilon & C_I^T \end{bmatrix} \begin{bmatrix} \Delta E_\varepsilon \\ \Delta T \end{bmatrix}, \quad (2)$$

where C_f^ε , C_f^T , C_I^ε и C_I^T are coupling coefficients for the corresponding parameters [8 – 11].

Typical values of these coefficients for G. 652 OF under normal conditions (at room temperature and without longitudinal strain) are as follows: $C_f^\varepsilon = 48 \text{ kHz}/\mu\varepsilon = 480 \text{ MHz}/\%$ (1 % of strain is equal to $10^4 \mu\varepsilon$), $C_f^T = 1.06 \text{ MHz}/^\circ\text{C}$, $C_I^\varepsilon = -8.07 \cdot 10^{-6}/\mu\varepsilon = -0.0807/\%$, $C_I^T = 0.0033/^\circ\text{C}$ [10 – 12]. C_f^ε is taken to be 493 MHz/% at room temperature according to the “Fujikura” [3, 4].

$$f_B(E_\varepsilon, T) = 2f_L v_A(E_\varepsilon, T) n_{ef} / c = 2v_A(E_\varepsilon, T) n_{ef} / \lambda_L. \quad (3)$$

where $v_A(E_\varepsilon, T)$ is the velocity of a hyperacoustic wave depending on the temperature, strain and core structure; n_{ef} is the effective refractive index of the medium, c is the velocity of light in vacuum [8 – 11].

Sensing the OF by short pulses the MBBS distribution along the optical waveguide is found. After the analysis of the distribution pattern of the MBBS in OF the f_B is determined (the values of MBBS peaks) along the OF ($f_B(E_\varepsilon)$).

It enables us to determine the strain degree of the OF and detect the location of the distributed irregularities in the OF by applying the MBBS $f_B(E_\varepsilon)$ dependence:

$$E_\varepsilon(z) = \frac{f_B(E_\varepsilon, z) - f_B(0)}{f_B(0) \cdot C_f^\varepsilon}, \quad \Delta E_\varepsilon(z) = \frac{\Delta f_B(z)}{f_B(0) \cdot C_f^\varepsilon}, \quad (4)$$

where $E_\varepsilon(z)$ is the dependence of OF strain on the longitudinal z coordinate along the OF; $\Delta E_\varepsilon(z)$ is the change in OF strain from the initial value; $f_B(E_\varepsilon, z)$ is the dependence of the frequency shift from the strain and z coordinate; $f_B(0)$ is the initial value of f_B ; $\Delta f_B(z)$ is the change of f_B from the z coordinate along the OF [1 – 4].

It is known that three points are necessary for unambiguous definition of the parabolic curve.

To accurately determine the f_B not just a frequency of received signal with a maximum of g_B is selected, but approximation in adjacent counts in the “peak” region is performed to estimate the MBBS maximum. Thus the square parabola passing through these counts is shaped. In the simplest case, the bandwidth at half power (–3 dB) of the maximum value is calculated for this parabola, and then the f_B is estimated as an average frequency of this range [4].

3. Improved algorithms for determining the Brillouin frequency shift

Fig. 3 shows a 3D-reflectogram BOTDR, which presents a distribution pattern of MBBS along the optical waveguide. The cross section of such 3D-reflectogram BOTDR along the longitudinal z coordinate is a reflectogram of OF at a fixed frequency. Along the frequency axis, each value of the longitudinal coordinate ($z = \text{const}$) determines the MBBS profile in this cross section [8 – 10].

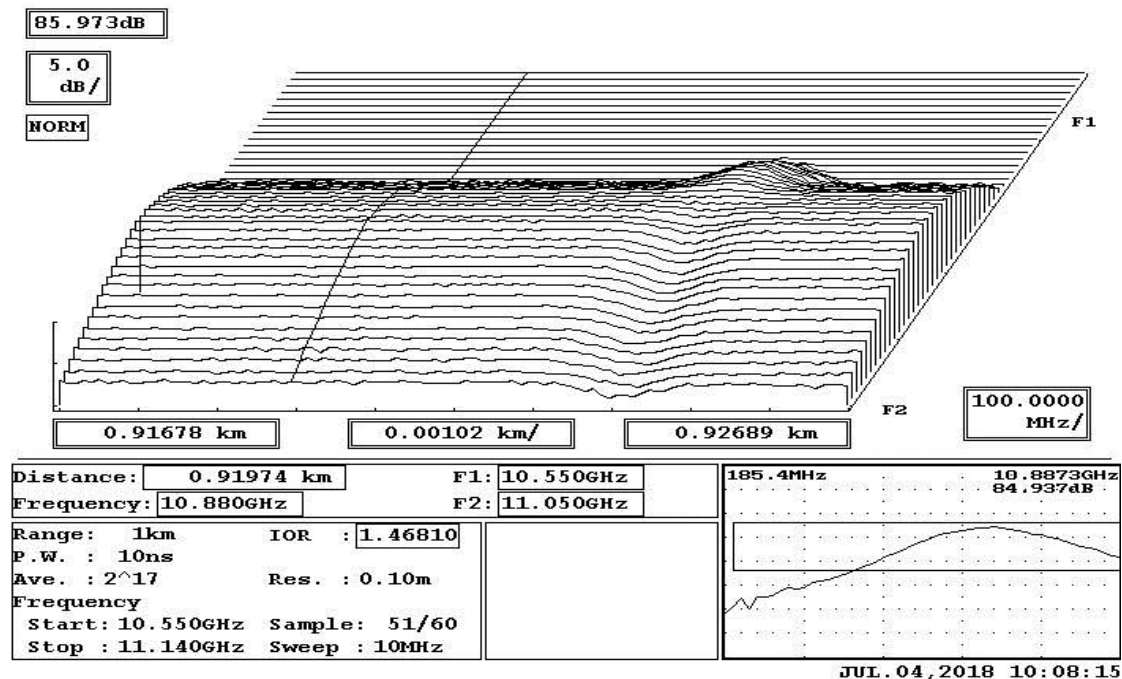


Figure 3. A 3D-reflectogram BOTDR – distribution patterns of MBBS along the optical waveguide

The lower right corner of the reflectogram shows both the MBBS maximum for a specific longitudinal coordinate and the response of MBBS profile in this cross section of the OF. For example, when the cross fiber section of $z = 919.7$ m the MBBS peak is observed at a frequency of 10.89 GHz with width of MBBS of 185.4 MHz and the signal level of 84.9 dB.

A core refractive index of the OF is $n = 1.4681$. The measurement accuracy in the longitudinal coordinate is 0.1 m. The real spatial resolution is 1 m for the probe pulse width of 10 ns.

The start frequency of the measurement range (F1) is 10.55 GHz, the stop (F2) is 11.14 GHz with a sweep frequency of 10 MHz. The number of averages is equal to 2^{17} .

Experience with the “Ando AQ 8603” has shown that the measurement process is very slow at high resolution.

In order to start the measurement we need to set the scan range with start (F1) and stop frequency (F2), as well as the sampling interval (Δf), which is equable and depends on both the specified number of measurement points (N) and the number of averages. This value is called “average time” in usual OTDR.

For example, the process of obtaining the reflectograms can take about one hour with 50 measurement points, the spatial accuracy of the reflectogram of 0.05 m and the number of averages of 2^{17} . Despite the fact that this time can be significantly reduced by applying smaller values, it remains significant in comparison with usual OTDR.

Typical values for the initial level (for normal conditions: at room temperature without mechanical strains) of the Brillouin frequency shift (f_{B0}) are obtained for the frequently used types of OF [12 – 14]. For standard single-mode OF (ITU-T recommendation G. 652) the f_{B0} is within 10.83...10.86 GHz. For frequently used types of OF the f_{B0} values can be used from the database [12 – 14] to determine the frequency scan range of the measured MBS signal.

The process of determining the MBBS maximum can be significantly accelerated by adapting the measurement one.

The analysis of the BOTDR-reflectogram shows that not all counts taken in the points of the reflectogram with a sampling interval (Δf) and a longitudinal coordinate (Δz) are of interest for obtaining the final result as presented in Fig. 3

Fig. 4 shows the explanation of the discussed algorithm of processing the BOTDR-reflectogram. N corresponds to the number of the current sample. $z_1 > z_2 > z_3 > z_4 > z_i >$ are the values in fixed (selected) cross sections (longitudinal coordinates ($z = \text{const}$)).

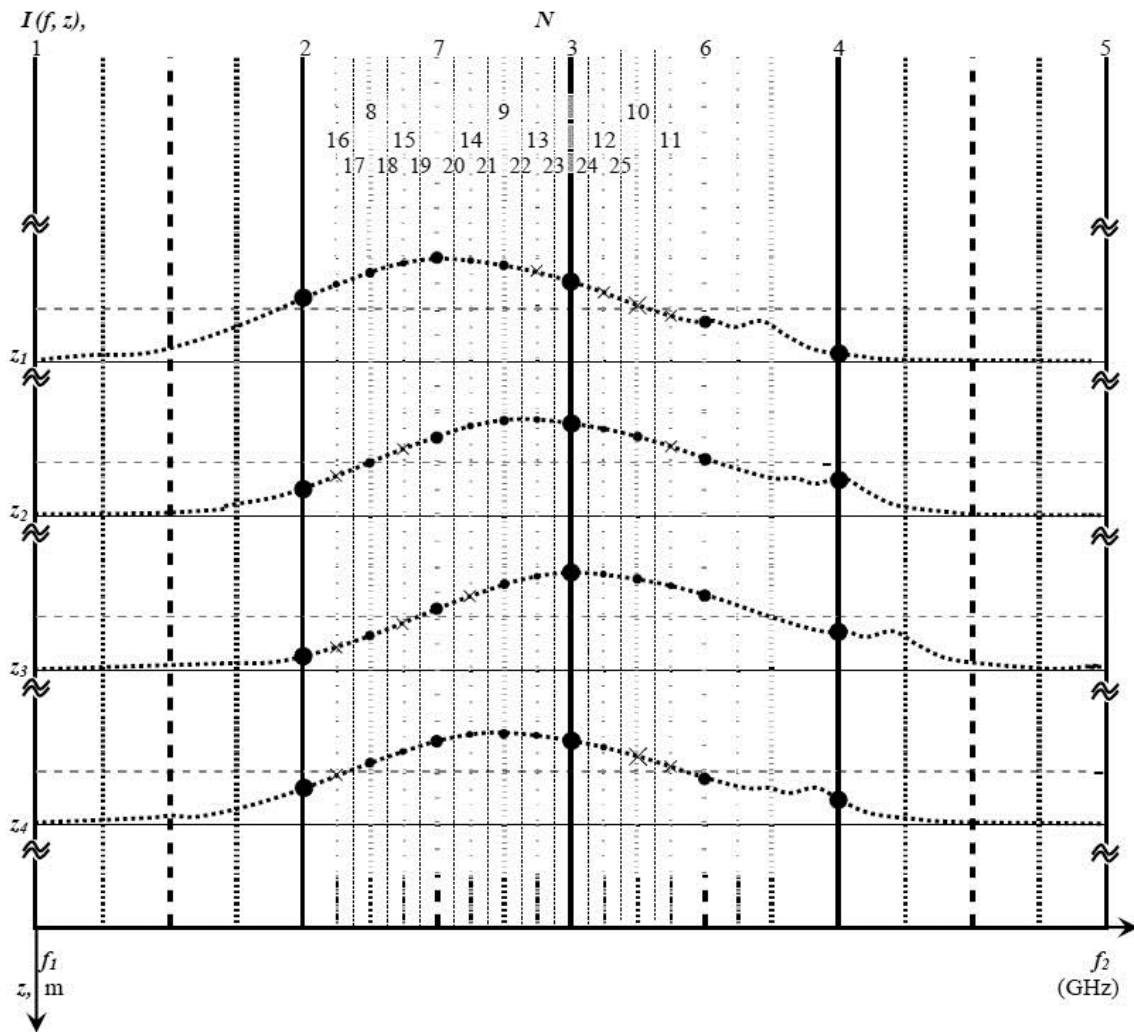


Figure 4. Selection of counts in the BOTDR-reflectogram with adaptive algorithm

At the initial step, the measurement range is divided into 4 identical parts with an interval of Δf_j : in addition to the start ($F1$) and stop ($F2$) frequencies, three more counts spaced from each other by the interval value are determined.

$$\Delta f_1 = (F2 - F1) / 4, \quad f_1 = F1, \quad f_2 = f_1 + \Delta f_1, \quad f_3 = f_1 + 2\Delta f_1, \quad f_4 = f_1 + 3\Delta f_1, \quad f_5 = F2. \quad (5)$$

After that, in each cross section the intensity of the backscattered signal $I(f, z)$ is determined and the peak value for the current counts (counts 1 – 5) is selected by a specified scanning interval along the longitudinal coordinate of z_i .

Then the sampling interval is reduced twice $\Delta f_2 = \Delta f_1 / 2$, but the following construction of reflectograms on the frequencies of the backscattered signal is carried out only in segments with signal

levels having power comparable to the peak level (less than 5 dB from the “peak”) for each cross section along the longitudinal z coordinate (counts 6 – 7).

The counts in the maximum region are necessary for further analysis (determination of f_B), and the counts with power less than 5 dB relative to the peak level are excluded from further process.

The “usable” counts are indicated by “points” in the MBBS profile, and the “unusable” counts for the definition of f_B are pointed by “crosses” as shown in Fig. 4.

In the same way the intensity of the backscattered signal $I(f, z)$ is determined for the obtained counts (6, 7), and the peak value is selected for all counts (1 – 7) achieved at this step for the current value of the longitudinal coordinate of z_i .

Then the process is repeated periodically at the new maximum region with a halved interval $\Delta f_i = \Delta f_{i-1} / 2$. It continues until the minimum interval is reached. The f_B value is then adjusted using the algorithms described above.

In Fig.4 the third step corresponds to the counts of 8 – 10, the fourth step is attributable to the counts of 11 – 16 and the fifth – to the counts of 17 – 25.

If the positions of the peaks are in various counts (for example, in sections of z_1 ($N = 7$) and z_3 ($N = 3$) in Fig. 4) for different values of the longitudinal z coordinate, then in each cross section of z_i only counts with power not lower than 5 dB from the maximum level are analyzed (indicated by “points” in Fig. 4), and other counts pointed by “crosses” in Fig. 4 are neglected.

The result of this algorithm is an essential acceleration of the process due to gapping and ignoring the counts, which do not affect the final result.

If the maximum is detected at some step of the process, then in parallel with the main process we can start the process of determining the OF strain based on the equation (4) and building a pattern of its distribution along the optical waveguide $E_\varepsilon(z)$. In the next steps, the calculations will be adjusted.

The pre-testing pattern of $E_\varepsilon(z)$ allows a skilled BOTDR user to interrupt the measurement process to make adjustments to the measurement settings (changing the scan range, the sampling interval and the resolution and distance of the measurement, etc.), which also reduce the testing time.

Another way to accelerate the determination process is an adaptive change in the accumulation time of measurement results (the number of averages). Firstly, (the first step of measurements, counts 1 – 5) a small number of averages is taken (for example, 2^{12}), in the next steps it increases (for example, $2^{13} - 2^{14}$, counts 6 – 10), and only in the maximum region the number of averages becomes the maximum for the specified conditions (for example, 2^{17} , counts 17 – 25).

Using as an option two or three parallel processing channels in the receiving path can accelerate the operation of the BOTDR as a whole. In this case, several counts will be determined simultaneously at each step of the calculation process.

4. Conclusion

The algorithms presented in this paper allow us to accelerate the process of obtaining the final results in the BOTDR due to the expulsion of unusable counts from the processing operations.

When the f_{B0} is used from a database of different types of OFs and companies [12 – 14], the rate and efficiency of measurements can be improved.

Calculating the approximate value of the MBBS maximum at the initial steps of the process, we can quickly realize a pre-testing pattern of the strain distribution in the OF.

Acknowledgments

The work was carried out with the financial support of the Ministry of Education and Science of the Russian Federation within the scope of the base part of a State Assignment within the sphere of scientific activity (Project No. 8.9334.2017/8.9).

The author would like to thank partners from CJSC “Moskabel–Fujikura” (Moscow) for assistance in carrying out the experiments with BOTDR “Ando AQ 8603”.

References

- [1] Lutchenko S S, Kopytov E Y and Bogachkov I V 2017 Assessment Of Fiber Optic Communication Lines Reliability With Account Of External Factors Influence, *Dynamics of Systems, Mechanisms and Machines, Dynamics 2017 : proceedings*, pp 1–5 DOI: 10.1109/Dynamics.2017.8239481
- [2] Bogachkov I V 2019 The detection of pre-crash sections of the optical fibers using the Brillouin reflectometry method *Journal of Physics: Conference Series* **1210** (2019) pp 1–11 DOI:10.1088/1742-6596/1210/1/012022
- [3] Listvin A V and Listvin V N 2005 Reflectometry of communication optical fibers *LESARart* (Moscow) 208 p
- [4] AQ 8603. Optical fiber strain analyzer. Instruction manual AS-62577 2001 *Ando Electric Co Ltd.* (Japan) 190 p
- [5] Viavi MTS/T-BERD 8000 – fiber sensing module DTSS module: user manual. – *Viavi Solutions* 94 p
- [6] Patent of Russia on the useful model 186277, G 01 N 21/27. Brillouin optical time domain reflectometer for monitoring optical fibers / Bogachkov I V, 2018135383/28(058291), publ. 09.10.2018
- [7] Patent of Russia on the useful model 186231, G 01 N 21/27. Optical Brillouin reflectometer / Bogachkov I V, 2018135635/28(058643), publ. 10.10.2018
- [8] Bogachkov I V 2018 Determination of mechanical stressed places of optical fibers in optical cables using Brillouin reflectometers *T-comm* **12, 12** pp 78–83 DOI 10.24411/2072-8735-2018-10205
- [9] Bogachkov I V, Trukhina A I and Gorlov N I 2019 Detection of optical fiber segments with mechanical stress in optical cables using Brillouin reflectometers *International Siberian Conference on Control and Communications (SIBCON–2019)* (Tomsk) pp 1–6 DOI: 10.1109/SIBCON.2019.8729601
- [10] Bogachkov I V 2017 Temperature Dependences of Mandelstam – Brillouin Backscatter Spectrum in Optical Fibers of Various Types *Systems of Signal Synchronization, Generating and Processing in Telecommunications (SINKHROINFO–2017)* (Kazan) pp 1–6 DOI: 10.1109/SINKHROINFO.2017.7997505
- [11] Belal M and Newson T P 2012 Experimental examination of the variation of the spontaneous Brillouin power and frequency coefficients under the combined influence of temperature and strain *Journal of Lightwave Technology* **30 8** pp 1250–1255
- [12] Bogachkov I V, Trukhina A I, Inivatov D P, Kireev A P and Gorlov N I 2019 A classification of optical fibers types on the spectrum profile of the Mandelstam – Brillouin backscattering *Journal of Physics: Conference Series* **1210** (2019) pp 1–6 DOI:10.1088/1742-6596/1210/1/012023
- [13] Bogachkov I V, Inivatov D P and Choban A G 2018 Program of automatically detection the type of optical fibers using Brillouin reflectograms *Certificate of registration of electronic resource N23734* (Russia, OmSTU) Publ. 14.08.2018
- [14] Bogachkov I V 2019 Program for classification of optical fiber kinds on Brillouin reflectograms *Certificate 2019610752 of state registration of computer programs.* – 2018662391, 07.11.2018 (Russia, OmSTU), Publ. 18.01.2019